ACS OMEGA

http://pubs.acs.org/journal/acsodf

Article

Titanium Dioxide/Phosphorous-Functionalized Cellulose Acetate Nanocomposite Membranes for DMFC Applications: Enhancing Properties and Performance

Randa E. Khalifa,* Ahmed M. Omer, Mohamed H. Abd Elmageed, and Mohamed S. Mohy Eldin

Cite This: *ACS Omega* 2021, 6, 17194−17202

Read Online

ACCESS | Metrics & More | Article Recommendations

ABSTRACT: This study intends to provide new TiO_2/phosphorous-functionalized cellulose acetate (Ph-CA) nanocomposite membranes for direct methanol fuel cells (DMFCs). A series of TiO_2/Ph-CA membranes were fabricated via solution casting technique using a systematic variation of TiO_2 nanoparticle content. Chemical structure, morphological changes, and thermal properties of the as-fabricated nanocomposite membranes were investigated by FTIR, TGA, SEM, and AFM analysis tools. Further, membranes' performance, mechanical properties, water uptake, thermal-oxidative stability, and methanol permeability were also evaluated. The results clarified that the ion-exchange capacity (IEC) of the developed nanocomposite membranes improved and reached a maximum value of 1.13 and 2.01 m_{eq}/g at 25 and 80 °C, respectively, using TiO_2 loading of 5 wt % compared to 0.6 and 0.81 m_{eq}/g for pristine Ph-CA membrane at the same temperature. Moreover, the TiO_2/Ph-CA nanocomposite exhibited excellent thermal stability with appreciable mechanical properties (49.9 MPa). The developed membranes displayed a lower methanol permeability of 0.98×10^{-16} cm^2 s^{-1} compared to 1.14×10^{-9} cm^2 s^{-1} for Nafion 117. The obtained results suggested that the developed nanocomposite membranes could be potentially applied as promising polyelectrolyte membranes for possible use in DMFCs.

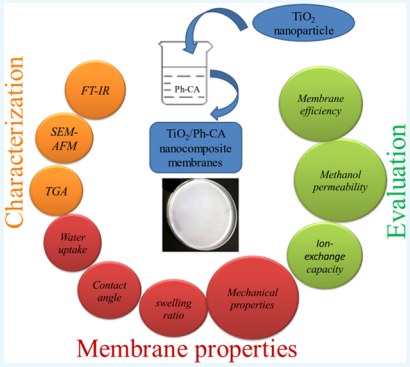

1. INTRODUCTION

As a proton conductive material, proton exchange membrane (PEM) is a critical part of the fuel cell system for transferring protons and acting as a barrier to fuel cross-leaks between the electrodes.[1] The most extensively used PEMs currently used in DMFC are the perfluorosulfonic acid type such as DuPont's Nafion.[2] Nafion exhibits high proton conductivity as well as good physical and chemical stabilities.[3,4] However, alternative nonperfluorinated materials[5−7] have been developed to overcome the drawbacks of Nafion such as high cost, low conductivity and stability at high temperatures, and methanol crossover.[8−11] Among these, cellulose derivatives have received much attention due to their low-cost production, availability, eco-friendliness, and ease of modification.[12−14] Cellulose acetate (CA) is commonly used to synthesize membranes due to its varied solubility in an extensive range of aprotic-polar organic solvent.[15] Cellulose acetate is a semicrystalline-thermoplastic insoluble in water but swells due to the existence of hydrophilic −OH and acetyl groups.[16] The CA membrane is also designated by better transport features and outstanding film-forming property with high hydrophilicity. CA has been physiochemically modified via cross-linking, grafting, sulfonation, amination, and composite formation to widen its applications range such as fuel cell,[17] water treatment, and desalination and biomedical fields.[18]

The polymeric−inorganic composite membranes have attracted significant attention owing to their dual functionality, such as specific chemical reactivity, mechanical properties, thermal stability of the inorganic backbone, and flexibility of the organic polymer backbone.[19] Among these inorganic materials, TiO_2 is considered a good hydrophilic filler for improving the mechanical properties and maintaining an appropriate hydration degree for the polymeric membranes.[20] Besides, TiO_2 has good compatibility with organic solvents, allowing the formation of homogeneous and stable dispersion without aggregation. Therefore, incorporating TiO_2 into the membrane matrix positively impacts their characteristics, due to its strong interaction with polymer structures.[21] Recently, organic/inorganic membrane composites have been considered for DMFC for increasing the cell performance, such as sulfonated SiO_2/sulfonated polyether sulfon,[22] sulfonated polysulfone/TiO_2,[23] sulfonated PAMPS/PSSA-TiO_2/SPEEK,[24] S-TaS_2/SPEEK,[25] etc.

Received: January 31, 2021
Accepted: June 15, 2021
Published: July 1, 2021

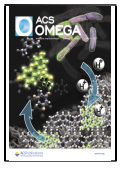

Herein, TiO_2/phosphorous-functionalized cellulose acetate (Ph-CA) nanocomposite membranes were successfully fabricated via the solution casting technique. The as-fabricated membranes were characterized using several characterization tools. Also, ion-exchange capacity, oxidative stability, mechanical properties, solvent uptake, and swelling were explored. Moreover, methanol crossover and performance were also evaluated.

2. RESULTS AND DISCUSSION

2.1. Size Analysis of TiO_2 NPs. The TiO_2 particle size distribution was estimated using a mixture of distilled water and ethanol as a solvent. The average particle size of TiO_2 was found to be 62 nm.

2.2. FTIR Analysis. FTIR spectroscopy was used to perceive the interactions between the functionalized CA and TiO_2 NPs. FTIR spectra of the native CA, Ph-CA membrane, and TiO_2/Ph-CA nanocomposite membranes with different NPs concentrations are shown in Figure 1. The results

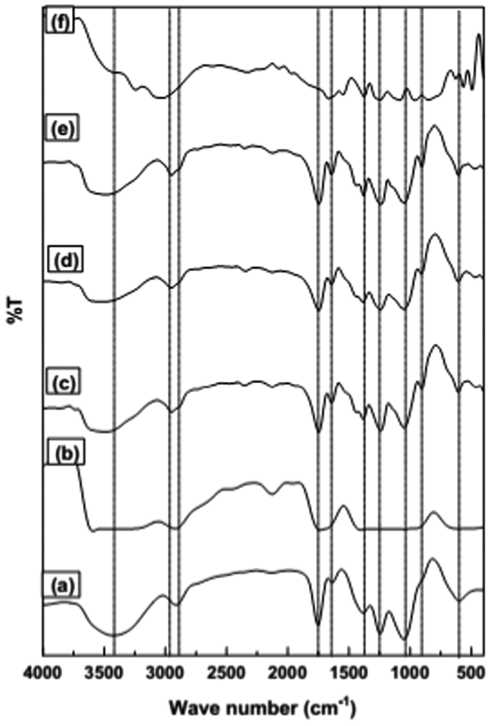

Figure 1. FTIR spectra of Ph-CA nanocomposite membranes with and without TiO_2 NPs: (a) native CA, (b) TiO_2/Ph-CA-0.0, (c) TiO_2/Ph-CA-2.5, (d) TiO_2/Ph-CA-5, (e) TiO_2/Ph-CA-7.5, and (f) TiO_2/Ph-CA-10.

indicated that the spectra of all of the tested samples have corresponding peaks of CA. It was observed that the synthesized nanocomposite membranes do not show any new peaks or a significant shifting of peaks. This behavior validates that TiO_2 NPs do not have chemical interactions with the functionalized polymer chains.[26] As shown in the figure, the observed absorption band at 3426 cm^{-1} in pure CA, which corresponds to OH− groups, was slightly shifted to a lower wavelength at 3414 cm^{-1} in Ph-CA due to the free OH− groups through the phosphorylation process. After the addition of TiO_2, the observed OH peak was shifted to a higher wavelength of 3484−3532 cm^{-1}. However, increasing TiO_2 NPs loading in the polymer matrix up to 10 wt % caused a decrease in the intensity of OH groups (3031 cm^{-1}). Besides, the peaks around 1753 cm^{-1} (for CA), 1755 cm^{-1} (for Ph-CA), and 1744−1746.6 cm^{-1} (for TiO_2/Ph-CA nanocomposites) were assigned to the stretching vibrations of the carbonyl group (C═O). The observed absorption bands at 1382.87, 1373, and 1384 cm^{-1} for CA, ph-CA, and TiO_2/Ph-CA nanocomposites were ascribed to the CH_3 bending vibration, respectively. The two peaks at 1230 and 1049 cm^{-1} in the spectrum of the ph-CA membrane assigned to the stretching vibrations C−O−C groups were slightly moved to 1239−1244.13 and 1047.38−1094.64 cm^{-1} in the nanocomposite membranes, respectively.

2.3. Morphological Changes. The surface morphology and cross section were examined by SEM analysis, as shown in Figure 2. The images clarified that the surface of native CA and Ph-CA membranes exhibited a smooth surface, and no cracks were found. Simultaneously, it changed to a roughly porous surface with irregular clusters and small granules in nanocomposite membranes.[27] Also, membranes with a lower concentration of TiO_2 NPs displayed denser structure (Figure 2c), while higher TiO_2 NP contents caused the more significant formation of macrovoids and more porous structures (Figure 2d,e). It was also noted that using surface modification and ultrasonication led to a decrease in the particle size and minimizing the particle agglomeration, which deduced the uniform dispersion of TiO_2 NPs. Likewise, the surface properties of nanosized TiO_2 composite materials have been investigated by others. Li et al.[28] reported that TiO_2 NPs were uniformly distributed with an irregular shape in the nanopacking film, improving the mechanical properties. Furthermore, Yoshiki et al.[29] stated the slightly rough surfaces of TiO_2 thin films with micro/NPs. Besides, the SEM images conducted by Zhu et al.[30] revealed the uniform incorporation of TiO_2 NPs in the chitosan-based coating membranes with uneven shapes.

The resulting micrographs of both two- and three-dimensional tapping mode of the developed nanocomposite membranes are illustrated in Figure 3. Figure 3a shows an AFM image for the pristine TiO_2/Ph-CA membrane (without TiO_2 fillers), with the dark region corresponding to the hydrophilic phosphonate groups (soft structure) and the bright phase being attributed to the hydrophobic polymer matrix (hard structure).[31] Figure 3b demonstrates an AFM image of the top surface morphology for the TiO_2/Ph-CA-5 nanocomposite membrane, reflecting the random distribution of TiO_2 NPs with some well dispersion and aggregates.[32] The presence of the filler in the nanocomposite membranes led to surface roughness, proportional to the concentration of filler added to the polymer matrix, and the surface roughness parameters were R_a = 5.96 nm and R_q = 7.88 nm for zero-loaded Ph-CA membrane and R_a = 13.73 nm and R_q = 17.32 nm for TiO_2/Ph-CA-5 nanocomposite membrane. However, when the TiO_2 content was 10 wt %, large aggregates or chucks occurred at an interface region with a layer structure. Consequently, the amount of polymer vs TiO_2 NPs should be controlled to obtain a well-dispersed and uniform nanocomposite membrane. From the images, it was clear that the compatibility between the polymer and TiO_2 is good.

2.4. Thermal Properties. Table 1 displays the thermal stability of the developed membranes. It was clear that native CA and Ph-CA membranes recorded a maximum weight loss of 4.61 and 8.46% at the ambient temperature (0−120 °C) due to water evaporation at the initial degradation stage. On the

https://doi.org/10.1021/acsomega.1c00568
ACS Omega 2021, 6, 17194−17202

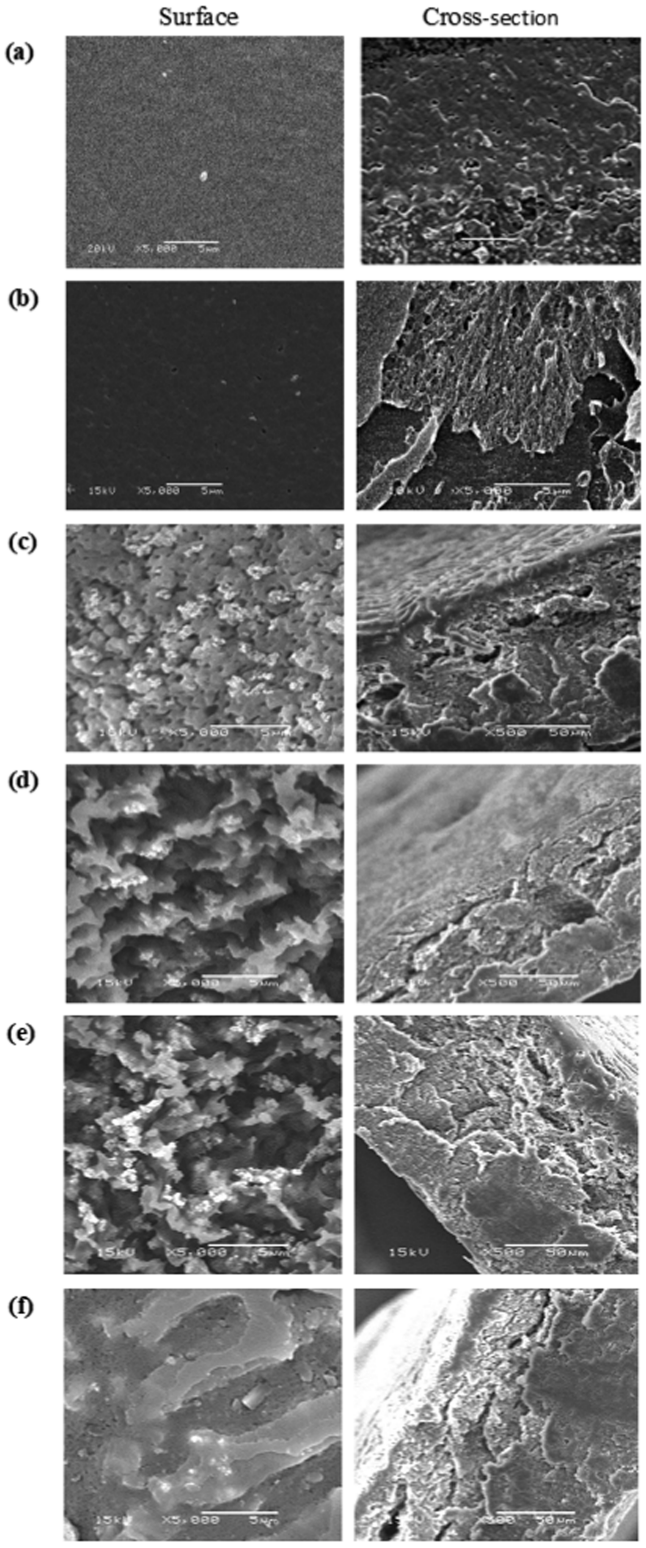

Figure 2. SEM images of (a) native CA, (b) TiO_2/Ph-CA-0.0, (c) TiO_2/Ph-CA-2.5, (d) TiO_2/Ph-CA-5, (e) TiO_2/Ph-CA-7.5, and (f) TiO_2/Ph-CA-10.

other hand, the weight loss increased with increasing TiO_2 content in the membrane matrix and reached maximum values ranging from 9.5 to 12.33% due to the high affinity of TiO_2 for trapping water molecules. In contrast, the developed nanocomposite membranes displayed better thermal stability with increasing temperature than native CA and Ph-CA. It was observed that the temperatures required for CA and Ph-CA to lose their half weights were 360.85 and 334.47 °C, while higher temperatures were needed in the case of nanocomposite membranes (i.e., 480−541 °C). Therefore, the entrapment of TiO_2 in the membrane matrix improved their thermal properties. These observations could be ascribed to the increase in membrane rigidity upon the addition of TiO_2 as a result of the strong interaction between the polymer chains and TiO_2 NPs.[33,34] These interactions are expected to delay the breakdown of CA chains and prevent the leaching of TiO_2 from the membrane matrix. Also, the probable coordination bond between Ti^{4+} and the acetate group of Ph-CA and the formation of hydrogen bonds among the accessible OH^- and acetate groups could be a reason for the higher thermal stability of the nanocomposite samples.[35]

2.5. IEC, Water Uptake, and Swelling Ratio. The most critical parameters in determining membranes' hydrophilic nature are water uptake (WU), swelling ratio, and IEC. Water acts as the carrier that transports protons through membranes, while excessive WU may lead to dimensional instability.[36] The water content (Table 2) of the nanocomposite membranes decreased with increasing the TiO_2 NP loading incorporation up to 10 wt %. These observations could be due to the distribution of the inorganic NPs that decrease the unoccupied volume and the swelling capability of the membrane.[37] The water uptake values were increased with increasing temperature from 25 to 80 °C due to the smooth penetration of water molecules into the membrane matrix, reflecting positively on their swelling aptitude. In agreement with these observations, Amjadi et al. declared comparable trends for the WU of composite membranes prepared from Nafion and SiO_2.[38] Amjadi et al. stated that WU increases with temperature owing to the increase in the specific volume. In amorphous polymers, mainly in temperatures closer to and above the polymer glass transition temperature (T_g), the free volume significantly influences the specific volume. Thus, a higher free volume induces greater water sorption.

It is well known that the electrochemical properties of the PEMs mainly depend on IEC and water uptake profiles.[39] Table 1 illustrates the values of experimental (IEC_{exp}) and calculated (IEC_{cal}, from the TGA curves) for the nanocomposite membranes upon the addition of TiO_2 NPs at 25 and 80 °C. It was clear that there was a slight change in the IEC value of the fabricated composite membrane compared with the TiO_2 free membrane. Similar to water uptake, increasing TiO_2 NP content from 5 to 10 wt % caused a decrease in the IEC_{exp} value from 1.13 to 0.82 m_{eq}/g at 25 °C and from 2.01 to 1.42 m_{eq}/g at 80 °C in TiO_2/Ph-CA-5 compared to TiO_2/Ph-CA-10 membrane due to the existence of a freer phosphonic group. Moreover, increasing the nanosized TiO_2 content covering the polymer backbone's active sites and reduces the adequate number of replaceable ion-exchangeable sites.[40]

Further, it was found that the ion-exchange process can be influenced by several factors, including the type of membranes, temperature, concentration, and pH. The results showed that the IEC changes vastly by increasing the temperature from 25 to 80 °C. This behavior may be explained by the increase in the specific volume and water absorption and by the fact that the affinity of the membrane increases with increasing charge (z) of the counterion because of the attractive electrostatic attraction among the counterions and functional groups. This phenomenon is called electroselectivity, and this affinity for the

https://doi.org/10.1021/acsomega.1c00568
ACS Omega 2021, 6, 17194−17202

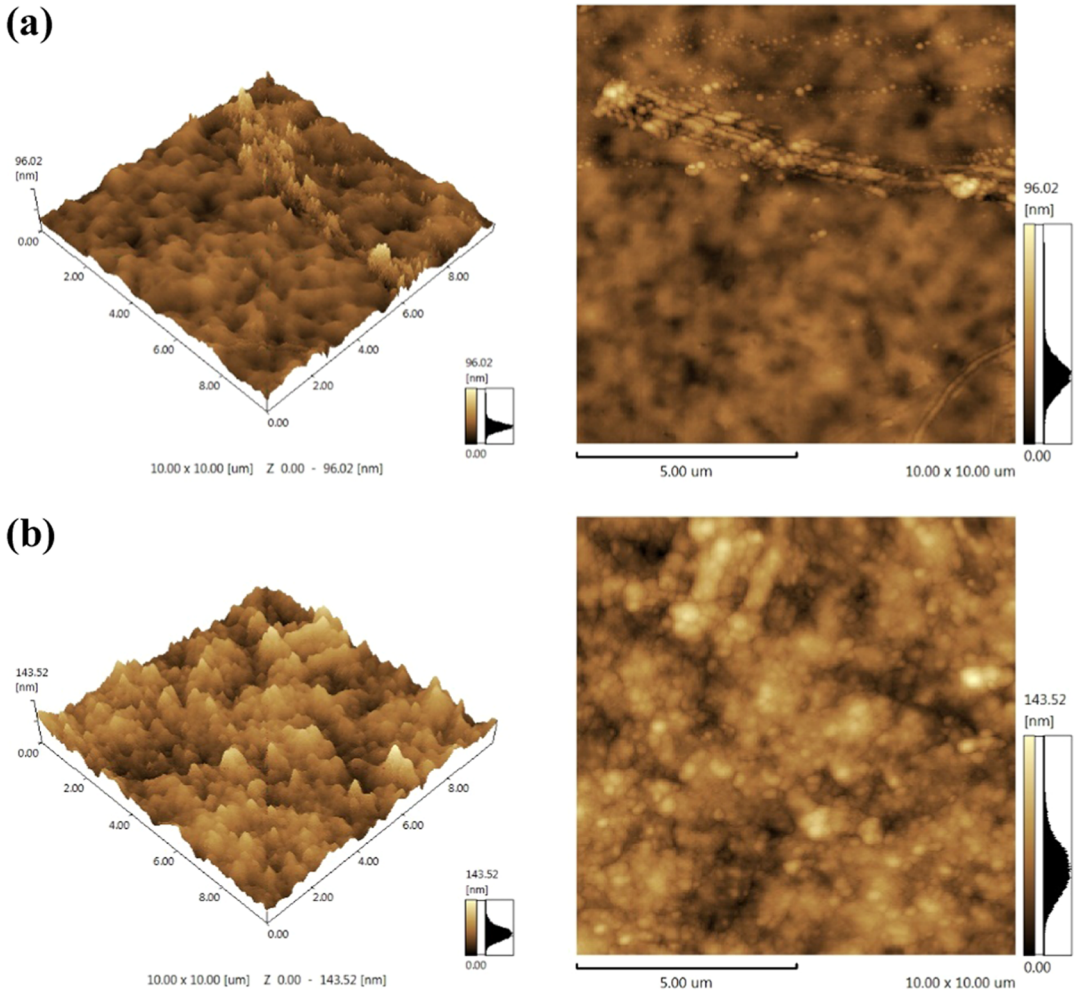

Figure 3. Two- and three-dimensional surface AFM images of (a) TiO_2/Ph-CA-0.0 and (b) TiO_2/Ph-CA-5 nanocomposite membrane.

Table 1. Weight Loss Percentage of TiO_2/Ph-CA Nanocomposite Membranes and IEC Values

sample code	weight loss (%) at ambient temperature (0−120 °C)	$T_{50\%}$ (°C)	IEC_{cal}/IEC_{exp} (25 °C)	IEC_{cal}/IEC_{exp} (80 °C)
CA	4.61	360.85	0.324/0.203	0.419/0.386
Ph-CA	8.46	334.27	0.629/0.6	0.849/0.81
TiO_2/Ph-CA-2.5	9.5	480.58	0.983/0.9	1.529/1.4
TiO_2/Ph-CA-5	10.12	520.06	1.436/1.3	2.320/2.1
TiO_2/Ph-CA-7.5	10.88	536.27	1.122/1.0	1.795/1.6
TiO_2/Ph-CA-10	12.33	541.34	0.912/0.8	1.482/1.3

Table 2. Swelling Ratio and Water Uptake of the Prepared TiO_2/Ph-CA Nanocomposite Membranes

	dimensional changes (ΔL %)		thickness changes (ΔT %)		water uptake (WU %)	
TiO_2 (wt %)	25 °C	80 °C	25 °C	80 °C	25 °C	80 °C
0	10.25	12.8	13.05	13.46	22.5	47.7
2.5	9.31	11.67	12.81	13.00	24.3	49.5
5	8.56	9.20	11.59	12.08	23.1	48
7.5	6.00	7.11	11.07	11.54	22.8	46.9
10	4.44	5.95	10.35	10.77	21	46.54

metal ions increases with increasing temperature. Other authors reported similar results.[41]

On the other hand, dimensional changes in the thickness and dimensions of the TiO_2/Ph-CA nanocomposite membranes were assessed in their dry state with the hydrated state. At the cathode side, membranes can interact with water when assembled in the FC system. Still, they can be swelled due to the absorbed water molecules that may affect protons' diffusional resistivity. Consequently, the ionic conductivity of the employed PEM could diminish. Thus, the measurements of swelling of TiO_2/Ph-CA membranes were examined at 25 and 80 °C. Table 2 reveals the decrease in the membrane swelling with increasing TiO_2 NP loading, which indicated that the swelling character is mainly influenced by the polymer nature and the polymer−solvent compatibility.[42] However, the swelling performance plays a notable role in mass transfer, ion exchange, and ionic interaction.[43]

2.6. Oxidative Stability and Mechanical Property. Thermal-oxidative stability is a crucial character for PEMs to achieve extended durability and a long working lifetime for the FC system.[44] For the nanocomposite membranes described above, oxidative stability was considered using hot Fenton's

https://doi.org/10.1021/acsomega.1c00568
ACS Omega 2021, 6, 17194−17202

reagent as an accelerated chemical degradation test to evaluate their stabilities against the radical species. This test was assessed for 12 and 24 h by measuring the weight loss as presented in Table 3. The results illustrated that the

Table 3. Accelerated Test Results of TiO_2/Ph-CA Nanocomposite Membranes

	retained weight (%)	
sample code	12 h	24 h
Ph-CA	67.00	58.70
TiO_2/Ph-CA-2.5	86.03	76.51
TiO_2/Ph-CA-5	89.46	79.79
TiO_2/Ph-CA-7.5	91.13	81.60
TiO_2/Ph-CA-10	91.80	82.92

nanocomposite membranes showed more stability after the addition of TiO_2 NPs owing to the role of TiO_2 in the interaction against the diffusion of H_2O_2.[45]

2.7. Contact Angle Analysis. The hydrophilic/hydrophobic behavior of the fabricated membranes can be specified by measuring their contact angle against water droplets. The contact angles of nanocomposite membranes in addition to the original CA and free loaded ph-CA membranes are tabulated in Table 4. Obviously, with the addition of TiO_2 nanoparticles,

Table 4. Contact Angle Measurement of TiO_2/Ph-CA Nanocomposite Membranes and Mechanical Properties

sample code	2θ	strain (%)
CA	47.04	2.64
Ph-CA	35.5	8.26
TiO_2/Ph-CA-2.5	33.2	7.75
TiO_2/Ph-CA-5	32.7	6.78
TiO_2/Ph-CA-7.5	37.7	4.45
TiO_2/Ph-CA-10	40.02	2.64
Nafion 117	110	12.2

the contact angle of the TiO_2/Ph-CA nanocomposite membranes was decreased from 35.5° for the pristine zero-laden Ph-CA membrane to 32.7° for the TiO_2/Ph-CA-5 membrane. On the other hand, a further increase in the TiO_2 content above 5 wt % causes a decrease in the hydrophilic character. This investigation supports that nanocomposite membranes demonstrated decent hydrophilic character, which indicates the clear phase separation between the cellulosic membrane and nanofiller.[26]

The mechanical properties of the membranes mentioned above were investigated to illustrate the effect of TiO_2 NPs on the membranes' performance stability in fuel cells. Thus, tensile strength (Figure 4) and elongation at break (Table 4) were determined. It was clear that the tensile strength was enhanced upon the addition of TiO_2 NPs in the synthesized membranes to reach a maximum value of 58 MPa at 7.5 wt % of TiO_2 compared to 37.7 and 18.2 MPa for zero-loaded membranes and Nafion. On the contrary, elongation at break was reduced from 8.26 to 2.64% due to the significant interaction between the nanofiller and functionalized cellulose acetate matrix. Further, the TiO_2 content increases up to 10 wt %, causing a marked decline in the membranes' tensile strength; since the filler at this content could not be uniformly dispersed, agglomeration occurred.[42]

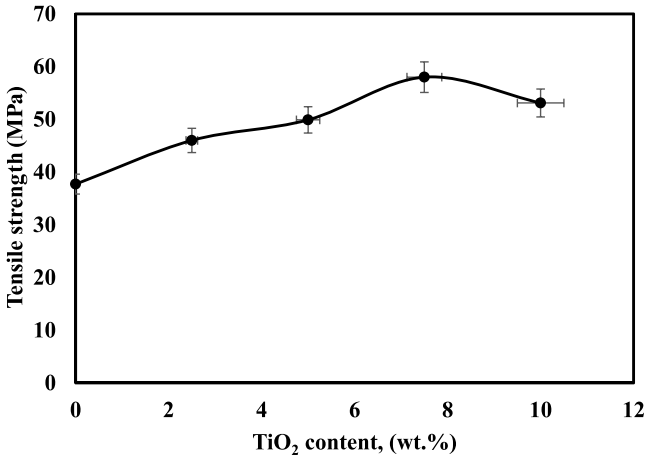

Figure 4. Mechanical properties of TiO_2/Ph-CA nanocomposite membranes.

2.8. Methanol Permeability. To further illustrate the possible use of the prepared TiO_2/Ph-CA nanocomposite membranes as PEMs, methanol permeability was measured at 25 °C. Figure 5 demonstrates the nanocomposite membrane's

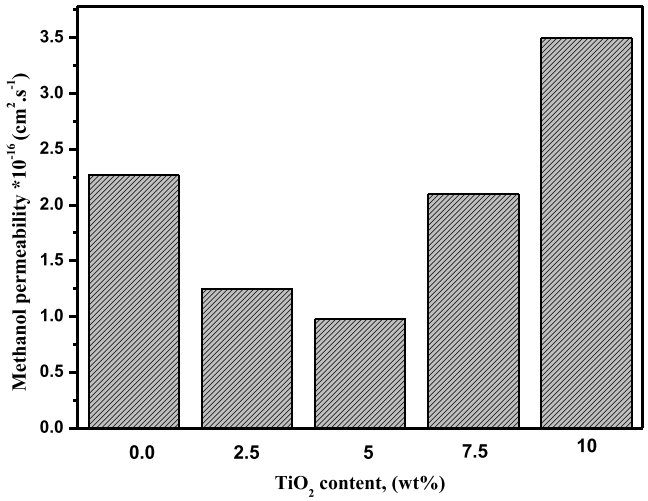

Figure 5. Methanol permeability of TiO_2/Ph-CA nanocomposite membranes.

methanol permeability coefficient with different TiO_2 contents than the Nafion membrane. The results clarified that methanol permeability decreased from 2.27×10^{-16} cm^2 s^{-1} for the plain membrane to 1.25×10^{-16} and 0.98×10^{-16} cm^2 s^{-1} for the TiO_2/Ph-CA-2.5 and TiO_2/Ph-CA-5 nanocomposite membranes, respectively. Lower methanol permeability proposes minor methanol crossover through the PEM, which indicates that the TiO_2/Ph-CA nanocomposite membranes could adequately protect the cathode catalyst from poisoning.

The methanol permeabilities of nanocomposite membranes with 7.5 and 10 wt % nanofiller contents were 2.1×10^{-16} and 3.5×10^{-16} cm^2 s^{-1}, respectively. A similar trend was stated by Jiang et al.[46] The higher methanol permeability of the TiO_2/Ph-CA-0.0 membrane than those of the TiO_2/Ph-CA-2.5 and TiO_2/Ph-CA-5 membranes may suggest that the holey-phosphonated structure could increase the interlayer spacing of the functionalized membrane, resulting in an increase in methanol diffusion through the membranes. Furthermore, at

https://doi.org/10.1021/acsomega.1c00568
ACS Omega 2021, 6, 17194−17202

lower TiO_2 NP contents (2.5, 5 wt %), the hydrophilic TiO_2 NPs primarily restricted the methanol crossover. In addition, TiO_2 NPs are likely involved in the cellulosic backbone (hydrophobic semicrystalline matrix) and caused aggregation of particles, which will alter the microstructure of the membrane and further change the methanol transport mechanism. The methanol permeation increased through the hydrophobic domains at higher TiO_2 contents (7.5, 10 wt %). In agreement with this result, Wu et al. reported a similar investigation.[44] These results suggest that the TiO_2/Ph-CA nanocomposite membranes could be used as the PEM with great potential to replace Nafion 117 (1.14×10^{-9} cm^2 s^{-1}).

2.8.1. Membrane Performance. Membrane efficiency is a direct indication of the membrane performance in DMFC. The efficiency factor as a function of TiO_2 NPs content at 25 °C is indicated in Figure 6. The results demonstrate that the

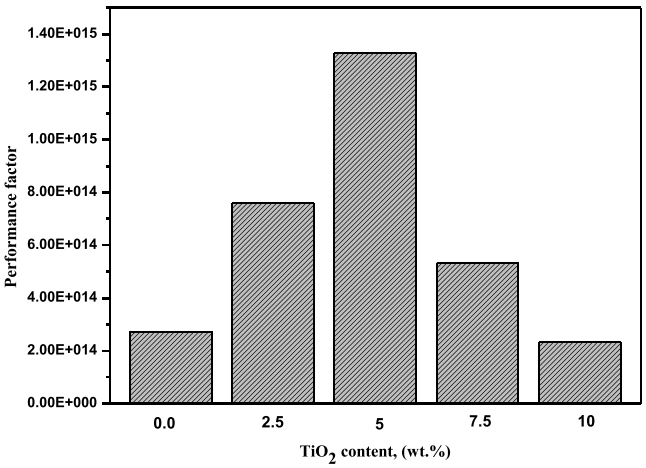

Figure 6. Performance factor as a function of TiO_2 NP content.

efficiency factor reaches a maximum peak at 5 wt % TiO_2 NPs load, which then decreases as the IEC decreased by a further increase in the TiO_2 NP content. Furthermore, the performance factor for all TiO_2/Ph-CA nanocomposite membranes was high compared to that of Nafion 117 as its performance efficiency is 2.6×10^5.

3. CONCLUSIONS

A series of TiO_2/Ph-CA nanocomposite membranes were successfully fabricated with various TiO_2 NPs as PEMs via the casting technique. Morphological analysis exhibits proper adhesion between the inorganic nanoparticle domains and the polymer matrix; thus, the surface morphology and mechanical properties were greatly improved. Characterization of the nanocomposite membranes using TGA proved their high thermal stability compared to the native and functionalized CA membranes. The results indicated that increasing the TiO_2 NP content up to 10 wt % in the TiO_2/Ph-CA nanocomposite membranes causes a decrease in the water uptake, swelling ratio, and IEC, i.e., the IEC reached its maximum value (1.13 m_{eq}/g) at 5 wt % TiO_2 concentration. Moreover, thermal-oxidative stability, mechanical properties, methanol permeability, and membrane performance were investigated to estimate their aptitude applicability in FC. It was clear that the entrapment of TiO_2 resulted in significant reductions in the methanol permeability compared to that of Nafion 117 membranes. Further, TiO_2/Ph-CA nanocomposite membranes showed the best cell performance associated with excellent thermal stability. Thus, the fabricated cost-effective nanocomposite membranes are predictable to be alternative candidates for the commercial Nafion membranes in DMFC applications. However, more long-term-based characteristics and performance are requisite assurance.

4. EXPERIMENTAL SECTION

4.1. Materials. Cellulose acetate (CA; degree of acetylation 40%), orthophosphoric acid (OPA; assay 98%), acetone (purity; 90%), epichlorohydrin (ECH; purity 99.5%), and titanium isopropoxide ($Ti(OiPr)_4$) were supplied by Sigma-Aldrich (Germany). Methanol (purity 99%) and ethanol (purity; 99.8%) were purchased from Fluka Chemie GmbH (Switzerland). Hydrochloric acid (assay; 37%) was provided by Polskie Odczynniki Chimiczne S.A. (Finland). Sodium chloride, sodium hydroxide, and hydrogen peroxide are analytical grades supplied by El-Gomhouria Co (Egypt).

4.2. Preparation of Nanosized TiO_2. Nanosized TiO_2 was synthesized by a sol−gel method.[47] In brief, $Ti(OiPr)_4$ (8 mL, 27 mmol) was dissolved in ethanol (82 mL) under nitrogen gas and then added dropwise at room temperature to a solution of ethanol/water (250 mL, 1:1 v/v) under constant stirring for 10 min. After that, the solution was filtered, and the obtained white precipitate was dried at 100 °C for 15 h.

4.3. Preparation of TiO_2/Ph-CA Nanocomposite Membrane. In a typical synthesis,[12] CA (10 wt %) was first dissolved in acetone and then activated with ECH (1:3 wt/v) for 12 h at 55 °C. The activated CA was then reacted with OPA (0.5 M) for 8 h in a water bath at 35 °C. After completing the reaction, appropriate amounts of TiO_2 nanoparticles (0.0, 2.5, 5.0, 7.5, and 10.0 wt %) were added to the functionalized polymer solution and mixed for 1 h in an ultrasonic bath. The resulting solution was cast in a glass Petri dish and dried overnight at 60 °C. The obtained membranes were washed several times with deionized water to eliminate the unreacted ECH and OPA and then stored in deionized water before testing. The nanocomposite membranes were coded as TiO_2/Ph-CA-0.0, TiO_2/Ph-CA-2.5, TiO_2/Ph-CA-5, TiO_2/Ph-CA-7.5, and TiO_2/Ph-CA-10, respectively.

4.4. Characterization and Membrane Properties. The nanoparticle size of TiO_2 was determined using a particle size analyzer (N5 submicron particle size analyzer, Beckman Coulter). The structural analysis of nanocomposite membranes was conducted using an FTIR spectrometer (Shimadzu FTIR-8400 S, Japan). The thermal stability of the membranes was investigated using a thermogravimetric analyzer (Shimadzu TGA-50, Japan) for a temperature range of 25−600 °C at a heating rate of 20 °C/min under nitrogen. Further, morphological changes were also examined using scanning electron microscopy (Joel Jsm 6360LA, Japan). The AFM device was a scanning probe microscope (Shimadzu SPM-9700). Small squares of the prepared membranes were cut and glued on glass substrate. The membrane surfaces were imaged in a scan size of 10 μm × 10 μm. The most used surface roughness parameters of the membranes, which are expressed in terms of the mean roughness (S_a) and root mean square of the Z data (S_q), were investigated.

4.4.1. Water Uptake and Swelling Ratio. Water uptake measurements were performed in batches at different temperatures by recording the weight changes between the dried and hydrated states. Before measurements, membranes with an area of 2 cm × 2 cm were dried in a vacuum oven at 120 °C for

https://doi.org/10.1021/acsomega.1c00568
ACS Omega 2021, 6, 17194−17202

24 h. Weighed dry films were then immersed in deionized water at 25 and 80 °C for 24 h till equilibrium. The additional water was carefully wiped off with tissue paper, and the membranes were then weighed directly. The experiments were conducted at least three times, and the results were expressed as mean values.

$$\text{WU}\ (\%) = \frac{W_w - W_d}{W_d} \times 100 \quad (1)$$

where W_d and W_w are the weights of membranes in the dry and hydrated states, respectively.

The dimensional stability of the nanocomposite membranes was assessed by immersing the films in water for 24 h at various temperatures.[48] The changes in thickness and length were calculated using the following equations

$$\text{thickness change}\ (\Delta T\ \%) = \frac{T_w - T_d}{T_d} \times 100 \quad (2)$$

$$\text{dimensional change}\ (\Delta L\ \%) = \frac{L_w - L_d}{L_d} \times 100 \quad (3)$$

where T_d and L_d are the thickness and length of the dry membranes, while T_w and L_w are the thickness and length measured in the hydrated state, respectively.

4.4.2. Ion-Exchange Capacity. The ion-exchange capacity (IEC) of the nanocomposite membranes was evaluated using classical acid−base titration.[12] Briefly, weighed membranes were immersed in NaCl solution (2 M) for at least 12 h at 25 and 80 °C to replace H^+ with Na^+. Then, the replaced protons were titrated with NaOH (0.1 M) using ph.ph as an indicator. IEC was determined as follows

$$\text{IEC}\ (m_{eq}/g) = V_{NaOH} \times \frac{C_{NaOH}}{W_d} \quad (4)$$

where V and C are the volume and concentration of the NaOH solution, respectively, and W_d is the membrane weight.

4.4.3. Oxidative Stability. Nanocomposite membrane of uniform size (2 cm × 2 cm) was soaked in Fenton's reagent (4 ppm $FeSO_4$ in 3% H_2O_2) at 80 °C. The oxidative stability was evaluated by recording the percentage of remains weight (RW %) after 12 and 24 h, where the Fenton's reagent changed every 10 h.[48]

4.4.4. Contact Angle Measurement. A contact angle meter (VCA 2500 XE equipped with a CCD camera and analysis software, AST Products, Billerica, MA) was utilized for investigating the wettability of the nanocomposite membranes by measuring its surface contact angle against water droplet at three different points within 20 s. A drop of water was carefully dropped on the sample surface, and the images were captured using the attached camera.

4.4.5. Methanol Permeability Measurements. The methanol permeability was determined employing a glass diffusion cell consisting of two identical compartments separated by the test membrane. One compartment (A) was filled with the feed (2 M methanol solution), and the other compartment (B) was charged with the permeate (deionized water), each with a volume of 100 mL. Before the test, the samples were soaked in deionized water for at least 24 h. Both compartments were kept magnetically agitated during the permeation experiment; 500 μL was withdrawn periodically at prescribed time intervals from the permeate compartment using a microsyringe, and the methanol concentration was measured vs time via an HPLC analyzer. All measurements were conducted at 25 °C, and the methanol permeability (P) was calculated from the slope of the linear plot of methanol concentration against permeation time as follows

$$P = \alpha \frac{V_B}{A} \times \frac{L}{C_A} \quad (5)$$

where α is the straight-line plot slope, V_B is the permeate volume, L is the sample thickness, and A is the membrane working area.

4.4.5.1. Membrane Efficiency Determination. DMFCs required PEMs with high proton conduction and less methanol permeability. The membrane performance assessment can be performed as follows

$$\phi = \frac{\sigma}{P} \quad (6)$$

where ϕ is a parameter that estimates the overall membrane performance in the ionic conductivity (σ) to methanol permeability (P) ratio. Herein, the IEC was used as an indicator for ionic conductivity. Thus, the performance of the TiO_2/Ph-CA nanocomposite membranes was compared with that of the original Ph-CA membrane and Nafion 117, according to the following equation[49,50]

$$\phi = \frac{\text{IEC}}{P} \quad (7)$$

4.4.6. Mechanical Properties. The tensile strength and elongation at break of the prepared nanocomposite membranes were measured at room temperature using the universal testing machine (Shimadzu UTM, Japan). Each sample (1.5 cm × 5 cm) was measured three times, and the mean values were reported at a constant 5 mm/min speed.

AUTHOR INFORMATION

Corresponding Author

Randa E. Khalifa − *Polymer Materials Research Department, Advanced Technologies and New Materials Research Institute (ATNMRI), City of Scientific Research and Technological Applications (SRTA-City), New Borg El-Arab City, Alexandria 21934, Egypt;* orcid.org/0000-0002-7972-3396; Phone: +20 128 246 7520; Email: randaghonim@gmail.com, rghonim@srtacity.sci.eg

Authors

Ahmed M. Omer − *Polymer Materials Research Department, Advanced Technologies and New Materials Research Institute (ATNMRI), City of Scientific Research and Technological Applications (SRTA-City), New Borg El-Arab City, Alexandria 21934, Egypt*

Mohamed H. Abd Elmageed − *Chemical Engineering Department, Faculty of Engineering, Alexandria University, Alexandria 21544, Egypt*

Mohamed S. Mohy Eldin − *Polymer Materials Research Department, Advanced Technologies and New Materials Research Institute (ATNMRI), City of Scientific Research and Technological Applications (SRTA-City), New Borg El-Arab City, Alexandria 21934, Egypt;* orcid.org/0000-0003-2228-211X

Complete contact information is available at: https://pubs.acs.org/10.1021/acsomega.1c00568

https://doi.org/10.1021/acsomega.1c00568
ACS Omega 2021, 6, 17194−17202

Author Contributions

The manuscript was written through contributions of all authors. All authors have given approval to the final version of the manuscript.

Notes

The authors declare no competing financial interest.

■ ACKNOWLEDGMENTS

The authors are thankful to the Polymer materials research department, Advanced Technologies and New Materials Research Institute (ATNMRI), City of Scientific Research and Technological Applications (SRTA-City), New Borg El-Arab City, for characterization and experimental facilities.

■ REFERENCES

(1) Ge, X.; He, Y.; Guiver, M. D.; Wu, L.; Ran, J.; Yang, Z.; Xu, T. Alkaline anion-exchange membranes containing mobile ion shuttles. *Adv. Mater.* **2016**, *28*, 3467−3472.

(2) Suda, Y.; Shimizu, Y.; Ozaki, M.; Tanoue, H.; Takikawa, H.; Ue, H.; Shimizu, K.; Umeda, Y. Electrochemical properties of fuel cell catalysts loaded on carbon nanomaterials with different geometries. *Mater. Today Commun.* **2015**, *3*, 96−103.

(3) Tsai, J. C.; Cheng, H. P.; Kuo, J. F.; Huang, Y. H.; Chen, C. Y. Blended Nafion/SPEEK direct methanol fuel cell membranes for reduced methanol permeability. *J. Power Sources* **2009**, *189*, 958−965.

(4) Lee, D. C.; Yang, H. N.; Park, S. H.; Kim, W. J. Nafion/graphene oxide composite membranes for low humidifying polymer electrolyte membrane fuel cell. *J. Membr. Sci.* **2014**, *452*, 20−28.

(5) Zhang, H.; Shen, P. K. A brief consideration about the structural evolution of perfluorosulfonic-acid ionomer membranes. *Int. J. Hydrogen Energy* **2012**, *37*, 4657−4664.

(6) Cui, Y.; Baker, A. P.; Xu, X.; Xiang, Y.; Wang, L.; Lavorgna, M.; Wu, J. Enhancement of Nafion based membranes for direct methanol fuel cell applications through the inclusion of ammonium-X zeolite fillers. *J. Power Sources* **2015**, *294*, 369−376.

(7) Omer, A. M.; Khalifa, R. E.; Tamer, T. M.; Elnouby, M.; Hamed, A. M.; Ammar, Y. A.; Ali, A. A.; Gouda, M.; Mohy Eldin, M. S. Fabrication of a novel low-cost superoleophilic nonanyl chitosan-poly (butyl acrylate) grafted copolymer for the adsorptive removal of crude oil spills. *Int. J. Biol. Macromol.* **2019**, *140*, 588−599.

(8) Hu, Y.; Yan, L.; Yue, B. Sulfonation mechanism of polysulfone in concentrated sulfuric acid for proton exchange membrane fuel cell applications. *ACS Omega* **2020**, *5*, 13219−13223.

(9) Sazali, N.; Salleh, W. N. W.; Jamaludin, A. S.; Razali, M. N. M. New perspectives on fuel cell technology: A brief review. *Membranes* **2020**, *10*, No. 99.

(10) Zhang, J.; Aili, D.; Lu, S.; Li, Q.; Jiang, S. P. Advancement toward polymer electrolyte membrane fuel cells at elevated temperatures. *Research* **2020**, 1−15.

(11) Jana, K. K.; Prakash, O.; Shahi, V. K.; Avasthi, D. K.; Maiti, P. Poly(vinylidene fluoride-co-chlorotrifluoro ethylene) nanohybrid membrane for fuel cell. *ACS Omega* **2018**, *3*, 917−928.

(12) Mohy Eldin, M. S.; Abd Elmageed, M. H.; Omer, A. M.; Tamer, T. M.; Yossuf, M. E.; Khalifa, R. E. Development of novel phosphorylated cellulose acetate polyelectrolyte membranes for direct methanol fuel cell application. *Int. J. Electrochem. Sci.* **2016**, *11*, 3467−3491.

(13) Mohy Eldin, M. S.; Abd Elmageed, M. H.; A, M.; Tamer, T. M.; Yossuf, M. E.; Khalifa, R. E. Novel proton exchange membranes based on sulfonated cellulose acetate for fuel cell applications: Preparation and characterization. *Int. J. Electrochem. Sci.* **2016**, *11*, 10150−10171.

(14) Mohy Eldin, M. S.; Abd Elmageed, M. H.; Omer, A. M.; Tamer, T. M.; Yossuf, M. E.; Khalifa, R. E. Novel aminated cellulose acetate membranes for direct methanol fuel cells (DMFCs). *Int. J. Electrochem. Sci.* **2017**, *12*, 4301−4318.

(15) Ghaemi, N.; Madaeni, S. S.; Alizadeh, A.; Daraei, P.; Vatanpour, V.; Falsafi, M. Fabrication of cellulose acetate/sodium dodecyl sulfate nanofiltration membrane: Characterization and performance in rejection of pesticides. *Desalination* **2012**, *290*, 99−106.

(16) Rana, D.; Scheier, B.; Narbaitzb, R. M.; Matsuuraa, T.; Tabe, S.; Jasim, S. Y.; Khulbe, K. C. Comparison of cellulose acetate (CA) membrane and novel CA membranes containing surface modifying macromolecules to remove pharmaceutical and personal care product micropollutants from drinking water. *J. Membr. Sci.* **2012**, *409*−*410*, 346−354.

(17) Torigoe, K.; Takahashi, M.; Tsuchiya, K.; Iwabata, K.; Ichihashi, T.; Sakaguchi, K.; Sugawara, F.; Abe, M. High-power abiotic direct glucose fuel cell using a gold-platinum bimetallic anode catalyst. *ACS Omega* **2018**, *3*, 18323−18333.

(18) Nadeem, M.; Yasin, G.; Arif, M.; Bhatti, M. H.; Sayin, K.; Mehmood, M.; Yunus, U.; Mehboob, S.; Ahmed, I.; Flörke, U. Pt-Ni@PC900 hybrid derived from layered-structure Cd-MOF for fuel cell ORR activity. *ACS Omega* **2020**, *5*, 2123−2132.

(19) Eltaweil, A. S.; Abd El-Monaem, E. M.; Omer, A. M.; Khalifa, R. E.; Abd El-Latif, M. M.; El-Subruiti, G. M. Efficient removal of toxic methylene blue (MB) dye from aqueous solution using a metal-organic framework (MOF) MIL-101 (Fe): isotherms, kinetics, and thermodynamic studies. *Desalin. Water Treat.* **2020**, *189*, 395−407.

(20) Baglio, V.; Blasi, A. D.; Aricò, A. S.; Antonucci, V.; Antonucci, P. L.; Fiory, F. S. Influence of TiO_2 nanometric filler on the behaviour of a composite membrane for applications in direct methanol fuel cells. *J. New Mater. Electrochem. Syst.* **2004**, *7*, 275−280.

(21) Lvov, S.; Chalkovaa, E.; Rybkaa, G.; Fedkina, M. V.; Wesolowskic, D. J.; Roelofsd, M. G. Nafion/TiO_2 composite membranes for PEM fuel cells operating at elevated temperature and reduced relative humidity. *ECS Trans.* **2006**, *3*, 73−82.

(22) Maryam, S. A. H.; Parisa, S.; Ahmad, B.; Sepideh, K.; Hossein, B.; Parisa, H. The effect of adding sulfonated SiO_2 nanoparticles and polymer blending onproperties and performance of sulfonated poly ether sulfone membrane: Fabrication and optimization. *Electrochim. Acta* **2019**, 875−890.

(23) Devrim, Y.; Erkan, S.; Baç, N.; Eroğlu, I. Preparation and characterization of sulfonated polysulfone/titanium dioxide composite membranes for proton exchange membrane fuel cells. *Int. J. Hydrogen Energy* **2009**, *34*, 3467−3475.

(24) Parisa, S.; Mehran, J.; Saeed, P.; Maryam, S. A. Z.; Khadijeh, H.; Mohammad, B. A. Novel proton exchange membranes based onproton conductive sulfonated PAMPS/PSSA-TiO2hybrid nano-particles and sulfonated poly (etherether ketone) for PEMFC. *Int. J. Hydrogen Energy* **2018**, 3099−3114.

(25) Hossein, B.; Leyla, N.; Sebastiano, B.; Ahmad, B.; Beatriz, M. G.; Parisa, S.; Khadijeh, H.; Sara, N.; Michele, S.; Lea, P.; Bing, W.; Reinier, O. N.; Zdeněk, S.; Vittorio, P.; Francesco, B. Functionalized metallic transition metal dichalcogenide (TaS2) for nanocomposite membranes in direct methanol fuel cells. *J. Mater. Chem. A* **2021**, *9*, 6368−6381.

(26) Nurkhamidah, S.; Rahmawati, Y.; Gunardi, I.; Alifiyanti, P.; Priambodo, K. D.; Zaim, R. L.; Muqni, W. E. Enhancing properties and performance of cellulose acetate/polyethylene glycol (CA/PEG) membrane with the addition of titanium dioxide (TiO2) by using surface coating method. *MATEC Web Conf.* **2018**, *156*, No. 08016.

(27) Xing, Y.; Li, X.; Guo, X.; Li, W.; Chen, J.; Liu, Q.; Xu, Q.; Wang, Q.; Yang, H.; Shui, Y.; Bi, X. Effects of different TiO2 nanoparticles concentrations on the physical and antibacterial activities of chitosan-based coating film. *Nanomaterials* **2020**, *10*, 1365−1384.

(28) Li, H.; Feng, L.; Lin, W.; Sheng, J.; Xin, Z.; Zhao, L.; Xiao, H.; Zheng, Y.; Hu, Q. Effect of nano-packing on preservation quality of Chinese jujube (*Ziziphus jujuba* Mill. var. inermis (Bunge) Rehd). *Food Chem.* **2009**, *114*, 547−552.

(29) Yoshiki, H.; Mitsui, T. TiO2 thin film coating on a capillary inner surface using atmospheric-pressure microplasma. *Surf. Coat. Technol.* **2008**, *202*, 5266−5270.

(30) Zhu, Y.; Allen, G. C.; Adams, J. M.; Gittins, D.; Heard, P. J.; Skuse, D. R. Statistical analysis of particle dispersion in a PE/TiO2 nanocomposite film. *Compos. Struct.* **2010**, *92*, 2203−2207.

https://doi.org/10.1021/acsomega.1c00568
ACS Omega 2021, 6, 17194−17202

(31) Balappa, B. M.; Mahadevappa, Y. K. Development of novel sulfonic acid functionalized zeolites incorporated composite proton exchange membranes for fuel cell application. *Electrochim. Acta* **2018**, 294−307.
(32) Chun-Chen, Y.; Ying-Jeng, L. Preparation of the acidic PVA/MMT nanocomposite polymer membrane for the direct methanol fuel cell (DMFC). *Thin Solid Films* **2009**, *517*, 4735−4740.
(33) Abedini, R.; Mousavi, S. M.; Aminzadeh, R. A novel cellulose acetate (CA) membrane using TiO2 nanoparticles: Preparation, characterization and permeation study. *Desalination* **2011**, *277*, 40−45.
(34) Kim, H. T.; Lee, C. H.; Shul, Y. G.; Moon, J. K.; Lee, E. H. Evaluation of PAN-TiO2 composite adsorbent for removal of Pb(II) ion in aqueous solution. *Sep. Sci. Technol.* **2003**, *38*, 695−713.
(35) Das, C.; Gebru, K. A. Cellulose acetate modified titanium dioxide (TiO2) nanoparticles electrospun composite membranes: fabrication and characterization. *J. Inst. Eng. Ser. E* **2017**, *98*, 91−101.
(36) Malinowski, M.; Iwan, A.; Parafiniuk, K.; Gorecki, L.; Pasciak, G. Electrochemical properties of PEM fuel cells based on Nafion-polybenzimidazole-imidazole hybrid membranes. *Int. J. Hydrogen Energy* **2015**, *40*, 833−840.
(37) Gómez, E. E. R.; Hernández, J. H. M.; Astaiza, J. E. D. Development of a Chitosan/PVA/TiO2 nanocomposite for application as a solid polymeric electrolyte in fuel cells. *Polymers* **2020**, *12*, 1−14.
(38) Amjadi, M.; Rowshanzamir, S.; Peighambardoust, S. J.; Sedghi, S. Preparation, characterization and cell performance of durable Nafion/SiO2 hybrid membrane for high-temperature polymeric fuel cells. *J. Power Sources* **2012**, *210*, 350−357.
(39) Al-Othman, A.; Nancarrow, P.; Tawalbeh, M.; Ka'ki, A.; El-Ahwal, K.; El Taher, B.; Alkasrawi, M. Novel composite membrane based on zirconium phosphate-ionic liquids for high temperature PEM fuel cells. *Int. J. Hydrogen Energy* **2021**, *46*, 6100−6109.
(40) Staiti, P.; Arico, A. S.; Baglio, V.; Lufrano, F.; Passalacqua, E.; Antonucci, V. Hybrid Nafion-silica membranes doped with heteropolyacids for application in direct methanol fuel cells. *Solid State Ionics* **2001**, *145*, 101−107.
(41) Akrem, C.; Fatma, G.; Islem, L.; Chiraz, H.; Béchir, H. Temperature effect on ion exchange equilibrium between CMX membrane and electrolytes solutions. *J. Water Reuse Desalin.* **2015**, *25*, 535−541.
(42) Devrim, Y. Preparation and testing of Nafion/titanium dioxide nanocomposite membrane electrode assembly by ultrasonic coating technique. *J. Appl. Polym. Sci.* **2014**, *131*, 1−10.
(43) Di Noto, V.; Bettiol, M.; Bassetto, F.; Boaretto, N.; Negro, E.; Lavina, S.; Bertasi, F. Hybrid inorganic-organic nanocomposite polymer electrolytes based on Nafion and fluorinated TiO^2 for PEMFCs. *Int. J. Hydrogen Energy* **2012**, *37*, 6169−6181.
(44) Wu, Z.; Gongquan, S.; Wei, J.; Hongying, H.; Suli, W.; Qin, X. Nafion and nano-size TiO_2−SO_4^{2-}solid superacid composite membrane for direct methanol fuel cell. *J. Membr. Sci.* **2008**, *313*, 336−343.
(45) Dias, F. G. D. A.; Veiga, A. G.; Andreopoulou, A. K.; Kallitsis, J. K.; Rocco, M. L. M. Spectroscopic Study of Reinforced Cross-Linked Polymeric Membranes for Fuel Cell Application. *ACS Omega* **2020**, *5*, 15901−15910.
(46) Jiang, R.; Kunz, H. R.; Fenton, J. M. Composite silica/Nafion(R) membranes prepared by tetraethylorthosilicate sol−gel reaction and solution casting for direct methanol fuel cells. *J. Membr. Sci.* **2006**, *272*, 116.
(47) Chen, X.; Mao, S. S. Titanium dioxide nanomaterials: Synthesis, properties, modifications and applications. *Chem. Rev.* **2007**, *107*, 2891−2959.
(48) Munavalli, B. B.; Naik, S. R.; Kariduraganavar, M. Y. Development of robust proton exchange membranes for fuel cell applications by the incorporation of sulfonated β-cyclodextrin into crosslinked sulfonated poly(vinyl alcohol). *Electrochim. Acta* **2018**, *286*, 350−364.
(49) Ru, C.; Gu, Y.; Na, H.; Li, H.; Zhao, C. Preparation of a Cross-Linked Sulfonated Poly(arylene ether ketone) Proton Exchange Membrane with Enhanced Proton Conductivity and Methanol Resistance by Introducing an Ionic Liquid-Impregnated Metal Organic Framework. *ACS Appl. Mater. Interfaces* **2019**, *11*, 31899−31908.
(50) Rikukawa, M.; Inagaki, D.; Kaneko, K.; Takeoka, Y.; Ito, I.; Kanzaki, Y.; Sanuia, K. Proton conductivity of smart membranes based on hydrocarbon polymers having phosphoric acid groups. *J. Mol. Struct.* **2005**, *739*, 153−161.

https://doi.org/10.1021/acsomega.1c00568
ACS Omega 2021, 6, 17194−17202